PERGAMON

International Journal of Heat and Mass Transfer 46 (2003) 101–111

International Journal of HEAT and MASS TRANSFER

www.elsevier.com/locate/ijhmt

Shape design for a cylinder with uniform temperature distribution on the outer surface by inverse heat transfer method

Chin-Hsiang Cheng *, Mei-Hsia Chang

Department of Mechanical Engineering, Tatung University, 40 Chungshan N. Road, Sec. 3, Taipei 10451, Taiwan, ROC

Received 4 March 2002; received in revised form 7 June 2002

Abstract

Performance of the inverse heat transfer method in application to the shape design for the heat convection problems has been evaluated. The approach is constructed by combining curvilinear grid generation scheme, direct problem solver, conjugate gradient optimization method, and redistribution method. Shape design for the outer surface profile of a solid medium in a crossflow that contains a heating element and features an isothermal outer surface has been carried out. Practical cases under different combinations of the dominant physical parameters, including Reynolds number (Re), thermal conductivity ratio (k_f/k_s), desired outer surface temperature (θ_d), and Prandtl number (Pr), are studied to evaluate the effects of the physical parameters on the shape design.

Keywords: Shape design; Inverse heat transfer; Optimization

1. Introduction

It is known that the space program, starting from about 1956, gave considerable impetus to the studies of the inverse heat transfer problems (IHTP). One of the earliest papers dealing with the IHTP was reported by Stolz [1] in 1960. The author calculated heat transfer rates during quenching of bodies of simple finite shapes. Considering semi-infinite geometries, Mirsepassi [2,3] had used a similar technique both numerically and graphically for several years prior to 1960. A Russian paper by Shumakov [4] on the IHTP was translated in 1957. Up to now, using the method of IHTP can successfully estimate the unknown boundary conditions, such as temperature [5], heat flux [6,7], internal heat generation [8], contact resistance [9], thermal properties [10,11] by utilizing the transient temperature measurements taken within the objects.

Recently, shape design problems constitute an important kind of IHTP problems, which are commonly encountered in a number of engineering applications. Practical applications of shape design range from the topological optimization for mechanical structures [12,13] to the design of fin shapes [14–17]. In general, the problems raised in the practical shape design applications are normally to find an optimal geometry for a heat transfer system to meet some specific heat transfer requirements. Solutions obtained in this kind of problems may significantly increase the accuracy of component design and hence improve the performance of the whole system. A poor design for the shape of components may result in heat accumulation in the devices and even cause damage.

Cheng and Wu [18] proposed an optimization process for designing the shape profile of a solid medium that features an isotherm outer surface, using the body-fitted grid generation and the conjugate gradient methods. In their study, attention was focused on the applications of the direct differentiation scheme for the sensitivity analysis and on the problems with simply connected domains. Lately, Cheng and coworkers [19] modified

* Corresponding author. Tel. +886-02-25925252x3410; fax: +886-02-25997142.

E-mail address: cheng@ttu.edu.tw (C.-H. Cheng).

0017-9310/03/$ - see front matter © 2002 Published by Elsevier Science Ltd.
PII: S0017-9310(02)00226-0

Nomenclature

$Bi(X)$	Biot number $[= h(x)L/k_s]$
$h(x)$	heat transfer coefficient
J	objective function
k_f	thermal conductivity of fluid
k_s	thermal conductivity of solid
L	length of heating substrate
N	dimensionless outward normal coordinate to the outer surface
Pr	Prandtl number $[= \nu/\alpha]$
Re	Reynolds number $[= u_0 L/\nu]$
s	coordinate along outer surface
S	dimensionless coordinate along outer surface
T_a	temperature of ambient fluid
T_d	desired outer surface temperature
T_f	temperature of fluid
T_s	temperature of solid medium
T_w	temperature on heating substrate surface
u_0	free stream velocity
x, y	Cartesian coordinates
X, Y	dimensionless Cartesian coordinates
X_d, Y_d	shape functions of designed surface profile
$X_{i,d}$, $Y_{i,d}$	coordinates of grid point i on designed surface

Greek symbols

α	thermal diffusivity
ε	relative error of temperature at point i on the outer surface
θ_d	desired dimensionless outer surface temperature
θ_f	dimensionless temperature of fluid
θ_s	dimensionless temperature of solid medium
ν	kinematic viscosity
ξ, η	dimensionless curvilinear coordinates
ψ	stream function
Ψ	dimensionless stream function
ω	vorticity
Ω	dimensionless vorticity

Subscripts

i, j	grid indices
n	iteration number
N	number of grid points in the ξ-direction
M	number of grid points in the η-direction

the optimization method presented by Cheng and Wu [18] by introducing a redistribution process. With the help of the redistribution method, the undesired twisted or out-of-alignment grid points were improved and the convergence was facilitated. As a result, the applicability of the shape design method was then extended to the problems with the multiply connected domains. However, note that in these studies [18,19], only the heat conduction problems are considered, and the distribution of the heat transfer coefficient (h) on the outer surface of the solid medium is assumed to be uniform. This constant-h assumption may produce appreciable error since for the fluid flow over a solid body, the heat transfer coefficient may not be uniform on the body surface but varied as a function of position. The distribution of the heat transfer coefficient is greatly dependent on the flow pattern of the fluid. Therefore, without the knowledge of flow field, the heat transfer rate on the surface of the solid body cannot be accurately evaluated.

Design of the shape for the outer surface leading to an isothermal condition is of great practical importance to a number of thermal and fluid devices, such as electronic packages, isothermal heaters, and micro-heat sinks. Overall thermal performance for these devices is influenced by the uniformity of the temperature on the outer surface of the systems. For the electronic packaging problems having a solid medium containing an internal heating element inside, the heat dissipated by the heating element is spread over the entire solid medium by conduction and then transferred across the outer surface of the solid medium to the ambient fluid by convection. When the uniformity of the surface temperature can be improved, the thermal stress produced by temperature gradients adjacent to the surface can then be greatly reduced in order to avoid thermal deformation of the electronic packages.

In theory, the outer surface temperature is dependent on the heat transfer rate and the flow pattern as well. Also, the physical properties and the geometrical configuration of the solid medium containing the heating element have subtle influence on the outer surface temperature distribution. Since the thermal performance of the solid medium is dependent on the shape and the size of the solid medium, an optimal shape design definitely leads to an improvement in the thermal performance of the component.

In this study, the inverse heat transfer approach for the shape design problem [18,19] is extended to the analysis for the convection problems. The physical model of the test problem is shown in Fig. 1. A heating substrate of length L is imbedded within a conductive solid medium and the surface of the heating substrate is fixed at a uniform high temperature T_w. The heat dissipated from the heating substrate is spread over the entire solid medium domain and then is transferred across the

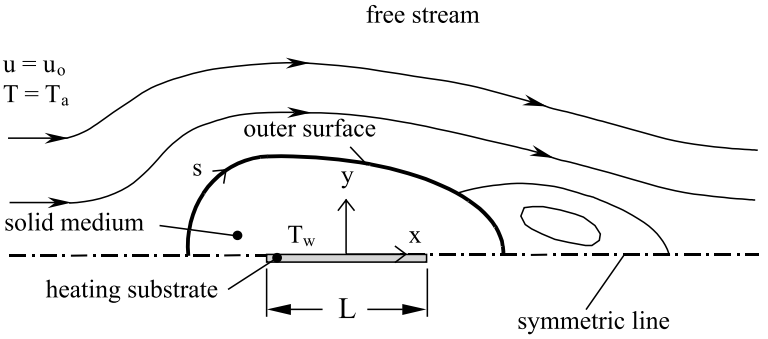

Fig. 1. Physical situation for shape design problem.

outer surface to the free stream by convection. Air stream at ambient temperature (T_a) flows over the solid medium with uniform velocity (u_0). The problem is stated as follows: It is desirable if heat transfer can be properly spread over the domain and as a result, the whole outer surface can be maintained at a uniform temperature. Magnitude of the desired outer surface temperature (T_d) may be specified arbitrarily but reasonably by the users. The objective of the study is thus to determine the shape for the solid medium that features an isothermal outer surface. It is expectable that the solution is dependent on the flow pattern of the fluid and also on the thermodynamic properties of the solid medium as well.

Three dominant dimensionless parameters are varied. The thermal and flow fields are assumed to be symmetric with respect to the x-axis herein. Based on the discussion on the wake vortex street behind a circular cylinder in crossflow given by Blevins [20], it is known that a symmetric wake vortex can exist only when the Reynolds number is less than approximately 40. Therefore, in this study the Reynolds number, representing quantitatively the velocity of the air flow, ranges from 5 to 40. This range of Reynolds number covers a wide range of air velocity particularly when the order of magnitude of the length of the heating substrate is reduced to the level of mini- or micro-meter. However, the methodology developed in this study is general and not limited to the symmetric flows and this range of Re.

The second parameter is the ratio of thermal conductivities, k_f/k_s, where k_f and k_s represent the thermal conductivities of fluid and solid medium, respectively. The value of k_f/k_s is assigned to be 0.05, 0.1, 0.2, 0.5 or 1.0. The third parameter, the desired dimensionless outer surface temperature (θ_d), is arbitrarily specified by the users and is varied the range $0 \leqslant \theta_d \leqslant 1.0$. The value of Prandtl number (Pr) is fixed at 0.71. Note that the outer surface profile of the solid medium containing the heating element can feature a required uniform temperature only when the shape of the solid medium is perfectly designed. A perfect design can only be predicted by means of a numerical optimization method which is robust and accurate.

2. Optimization methods

2.1. Direct problem solver

For the test problem shown in Fig. 1, the analysis is simplified as a two-dimensional, steady-state problem. The fluid properties are assumed constant, and the flow field is considered to be laminar. For fluid region, laws of conservation in mass, momentum, and energy equation can be expressed by using the stream function-vorticity formulation as

$$\frac{\partial^2\psi}{\partial x^2}+\frac{\partial^2\psi}{\partial y^2}=-\omega \tag{1}$$

$$u\frac{\partial\omega}{\partial x}+v\frac{\partial\omega}{\partial y}=\nu\left(\frac{\partial^2\omega}{\partial x^2}+\frac{\partial^2\omega}{\partial y^2}\right) \tag{2}$$

$$u\frac{\partial T_f}{\partial x}+v\frac{\partial T_f}{\partial y}=\alpha\left(\frac{\partial^2 T_f}{\partial x^2}+\frac{\partial^2 T_f}{\partial y^2}\right) \tag{3}$$

where ω and ψ represent the vorticity and the stream function of the fluid, respectively, which are defined by

$$\omega=\frac{\partial v}{\partial x}-\frac{\partial u}{\partial y} \tag{4a}$$

and

$$u=\frac{\partial\psi}{\partial y} \tag{4b}$$

$$v=-\frac{\partial\psi}{\partial x} \tag{4c}$$

and T_f is the temperature of fluid. Meanwhile, the steady-state heat conduction equation for the solid region can be given as

$$\frac{\partial^2 T_s}{\partial x^2}+\frac{\partial^2 T_s}{\partial y^2}=0 \tag{5}$$

where T_s represents the solid temperature.

The numerical grid generation method proposed by Thompson et al. [21,22] is employed to generate a curvilinear coordinate in terms of ξ and η. The solution domain consists of the solid and the fluid regions. Therefore, two independent sub-grids are required for the respective regions. For the fluid region, a multiple-block grid similar to that used by Yang et al. [23] is employed. The extent of the solution domain is determined such that the numerical solutions are independent of the extent of the solution domain. The multiple-block grid system obtained is shown in Fig. 2. Typically, the downstream region is extended to a distance 40 times the length of the solid medium. The shape of the solid region will be altered during the iterative shape design process. A new multiple-block grid system is generated for each iteration to accommodate the variation of the shape of the solid medium. Based on the curvilinear grid obtained, the governing equations, coupled with the boundary conditions, are then transformed, discretized, and solved in the computation domain (ξ, η).

By introducing the following group of dimensionless parameters,

$$X = \frac{x}{L}, \quad Y = \frac{y}{L}, \quad U = \frac{u}{u_0}, \quad V = \frac{v}{u_0}, \quad \theta = \frac{T - T_a}{T_w - T_a}$$

$$\Psi = \frac{\psi}{u_0 L}, \quad \Omega = \frac{wL}{u_0}, \quad Re = \frac{u_0 L}{\nu}, \quad Pr = \frac{\nu}{\alpha}, \quad Bi = \frac{hL}{k_s} \tag{6}$$

the transformed governing equations are derived from Eqs. (1)–(3) and (5), respectively, as

$$\bar{\alpha}\Psi_{\xi\xi} - 2\bar{\beta}\Psi_{\xi\eta} + \bar{\gamma}\Psi_{\eta\eta} = -Ja^2\Omega - Ja^2(F_1\Psi_\xi + F_2\Psi_\eta) \tag{7}$$

$$(\bar{u}\Omega)_\xi + (\bar{v}\Omega)_\eta = \frac{1}{ReJa}(\bar{\alpha}\Omega_{\xi\xi} - 2\bar{\beta}\Omega_{\xi\eta} + \bar{\gamma}\Omega_{\eta\eta}) + \frac{Ja}{Re}(F_1\Omega_\xi + F_2\Omega_\eta) + \Omega(\bar{u}_\xi + \bar{v}_\eta) \tag{8}$$

$$(\bar{u}\theta_f)_\xi + (\bar{v}\theta_f)_\eta = \frac{1}{RePrJa}(\bar{\alpha}\theta_{f\xi\xi} - 2\bar{\beta}\theta_{f\xi\eta} + \bar{\gamma}\theta_{f\eta\eta}) + \frac{Ja}{RePr}(F_1\theta_{f\xi} + F_2\theta_{f\eta}) + \theta(\bar{u}_\xi + \bar{v}_\eta) \tag{9}$$

$$\bar{\alpha}\theta_{s\xi\xi} - 2\bar{\beta}\theta_{s\xi\eta} + \bar{\gamma}\theta_{s\eta\eta} = -Ja^2(F_1\theta_{s\xi} + F_2\theta_{s\eta}) \tag{10}$$

where $\bar{u} = Y_\eta U - X_\eta V$, $\bar{v} = -Y_\xi U + X_\xi V$, $\bar{\alpha} = X_\eta^2 + Y_\eta^2$, $\bar{\beta} = X_\xi X_\eta + Y_\xi Y_\eta$, $\bar{\gamma} = X_\xi^2 + Y_\xi^2$, $Ja = X_\xi Y_\eta - X_\eta Y_\xi$, and F_1 and F_2 are two functions which are defined to artificially adjust the density of the grids locally. The above partial

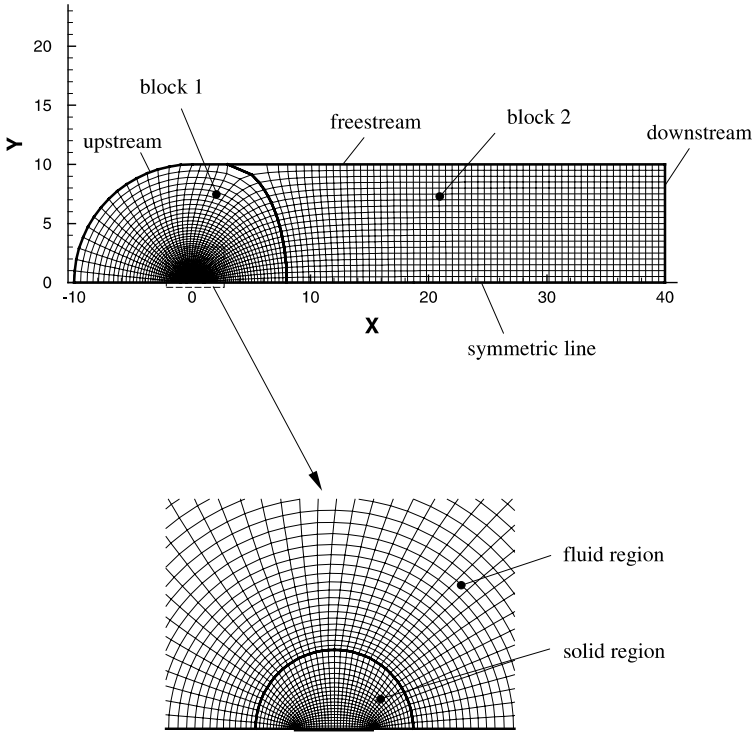

Fig. 2. Multiple-block grid system.

differential operators are defined by $()_\xi = \partial()/\partial\xi$, $()_{\xi\xi} = \partial()^2/\partial\xi^2$, $()_\eta = \partial()/\partial\eta$, and $()_{\eta\eta} = \partial^2()/\partial\eta^2$.

In the study, the convection and diffusion terms of Eqs. (8) and (9) are discretized with the power-law scheme described by Patankar [24]. The dimensionless boundary conditions associated with these above equations are

Fluid region:

$$\Omega = 0, \quad \Psi = Y, \quad U = 1, \quad V = 0 \quad \text{and} \quad \theta_f = 0 \quad \text{at upstream} \tag{11a}$$

$$\Omega = 0, \quad \Psi = Y_{max}, \quad U = 1, \quad V = 0 \quad \text{and} \quad \theta_f = 0 \quad \text{at freestream} \tag{11b}$$

$$\Omega_\xi = 0, \quad \Psi_\xi = 0, \quad U_\xi = 0, \quad V_\xi = 0 \quad \text{and} \quad \theta_{f\xi} = 0 \quad \text{at downstream} \tag{11c}$$

$$\Omega = 0, \quad \Psi = 0, \quad U_\eta = 0, \quad V = 0 \quad \text{and} \quad \theta_{f\eta} = 0 \quad \text{on symmetric line} \tag{11d}$$

$$\Omega = -(Y_\xi V_\eta + X_\xi U_\eta)/Ja, \quad \Psi = 0, \quad U = 0 \quad \text{and} \quad V = 0 \quad \text{at solid outer surface} \tag{11e}$$

Solid region:

$$\theta_s = 1 \quad \text{at surface of imbedded heating object} \tag{12a}$$

$$\theta_{s\xi} = 0 \quad \text{on symmetric line} \tag{12b}$$

Outer surface of solid medium:

$$\theta_f = \theta_s \quad \text{and} \quad -\frac{\partial\theta_s}{\partial N} = -\frac{\partial\theta_f}{\partial N}\left(\frac{k_f}{k_s}\right) \tag{13}$$

The coordinates of the grid points on the outer surface of the solid medium, $X_{i,d}(\xi)$ and $Y_{i,d}(\xi)$, are updated during the iteration optimization process. Based on the updated outer surface grids, a new sub-grid is generated for the solid region and another new multiple-block subgrid is generated for the fluid region. With the help of Eqs. (7)–(13), the flow field and the temperature distributions for both solid and liquid regions can be predicted.

2.2. Conjugate gradient optimization method

The shape profile of the medium domain represented by the outer surface grids is varied in order that the objective function, defined by

$$J = \sum_{i=1}^{N}(\theta_{si,M} - \theta_d)^2 \tag{14}$$

is minimized, where $\theta_{si,M}$ is the iterative dimensionless temperature at outer surface grid point i and θ_d is the desired outer surface temperature defined by

$$\theta_d = (T_d - T_a)/(T_w - T_a) \tag{15}$$

Minimization of the objective function J is achieved by using the conjugate gradient optimization method [18,19]. The conjugate gradient method evaluates the gradients of the objective function and sets up a new conjugate direction for the updated solutions with the help of a sensitivity analysis. In general, in a finite number of iterations the convergence can be attained. General descriptions and further details of the conjugate gradient optimization method are available in Refs. [18,19].

Based on the conjugate-gradient scheme, the coordinates of all grid points on the outer surface are updated until an optimal shape profile satisfying the convergence criterion is obtained. In a typical case, the convergence criterion for shape design is set with $J < 1.0 \times 10^{-5}$.

2.3. Redistribution method

The redistribution method proposed by Lan et al. [19] starts from detection of the ill-ordered grids during the optimization process. It is based on the assumption that the shape profile of the designed surface ought to be a smooth and continuous curve in physical reality. Thus, the ill-ordered grid patterns, such as twisted or out-of-alignment grids, are not desirable. Four major steps are included in the redistribution method: (1) detection, (2) alignment, (3) segmentation, and (4) redistribution. This method has also been found to be useful in improving the convergence of the optimal shape profile.

2.4. Numerical procedures

The sequence of the iterative optimization process in search of the desired shape profile can be summarized as:

(1) Prescribe all the boundary conditions and specify a desired reasonable outer surface temperature.
(2) Make an initial guess for the outer profile.
(3) Generate two sub-grids for solid and fluid regions that accommodate the latest outer profile.
(4) Solve Ω, Ψ, θ_f, and θ_s on the curvilinear computation domain.
(5) Calculate the objective function J by Eq. (14). When the objective function reaches a minimum, the solution process is terminated. Otherwise, go to step (6).
(6) Perform the sensitivity analysis.
(7) Calculate the conjugate gradient coefficient.
(8) Calculate the step size.
(9) Update the domain shape.
(10) Detect the ill-ordered outer surface grids, redistribute all the outer surface grids, and go to step (3).

3. Results and discussions

Firstly, the performance of the direct problem solver, which is used to solve the flow field and the temperature

distributions for the solid and the fluid regions, has been checked. Numerical checks for the direct problem solver are displayed in Fig. 3. Note that the grid systems used in the present study involve a 41×101 multiple-block grid system for the fluid region as well as a 41×21 grid system for the solid region. Fig. 3 shows the comparison between the present direct-problem solutions and the predictions provided by Dennis and Chang [25] for the flow over a circular cylinder at $Re = 5$, 10, and 20. Basically, good agreement between the two sets of data is observed. Note that Dennis and Chang [25] employed a cylindrical grid system which is different from the curvilinear grid system used in the present study. The slight difference between the two sets of data at $Re = 20$ may be attributed to the difference in grid systems and the number of grids used.

A grid-independence check has been made to ensure the accuracy of the numerical schemes. For this purpose, two grid systems are tested. The first grid system involves 41×21 grids for the solid region and 41×101 grids for the fluid region. The second grid system involves 81×41 grids for the solid region and 81×201 grid for the fluid region. The comparison in flow pattern yielded by these two grid systems is checked. For the cases at $Re = 20$ and $Pr = 0.71$, the grid-independence checks are shown in Fig. 4. It is found that the shape design is not sensitive to the change of grid number between the two grid systems. However, the computation time required is much longer on the grid system with 81×41 (solid)/81×201 (fluid) grid points than on that with 41×21 (solid)/41×101 (fluid) grid points.

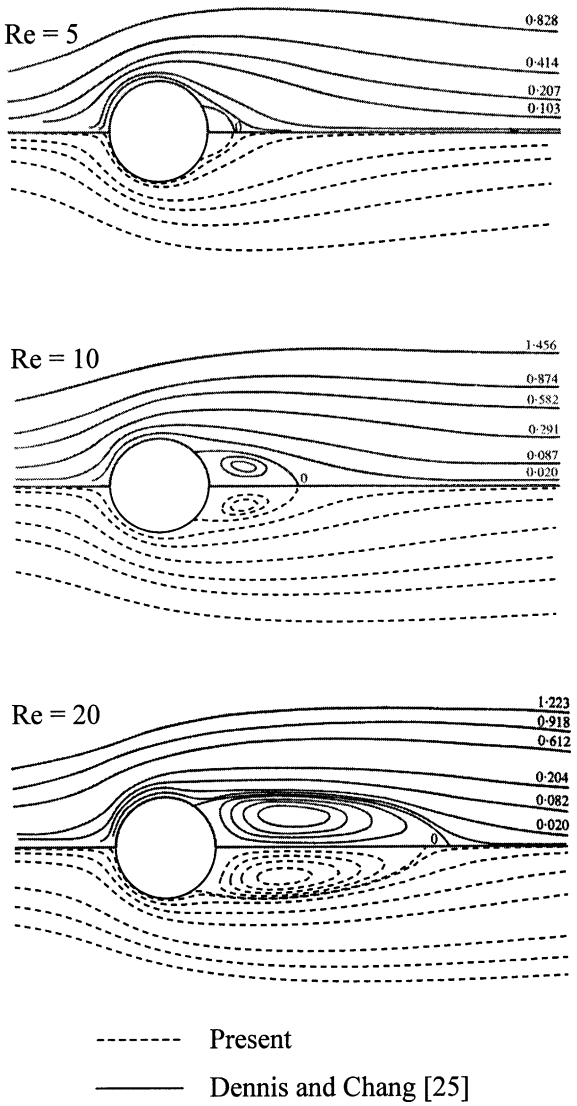

Fig. 3. Comparison between the present direct-problem solutions and the predictions of Dennis and Chang [25] for the flow over a circular cylinder at $Re = 5$, 10, and 20.

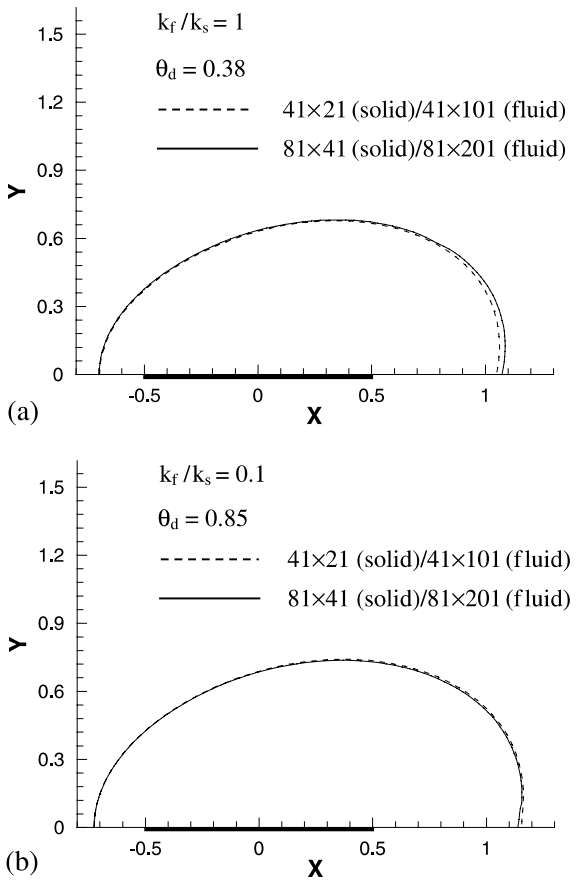

Fig. 4. Insensitivity of the designed shape to the grid size, for the case at $Re = 20$ and $Pr = 0.71$. (a) $k_f/k_s = 1$ and $\theta_d = 0.38$; (b) $k_f/k_s = 0.1$ and $\theta_d = 0.85$.

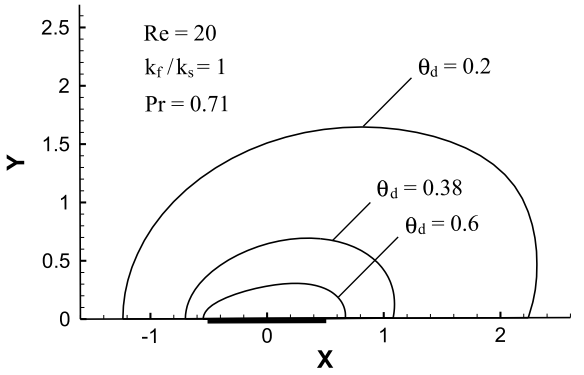

Fig. 5. Effects of the desired outer surface temperature on shape design, at $Re = 20$, $k_f/k_s = 1$, and $Pr = 0.71$.

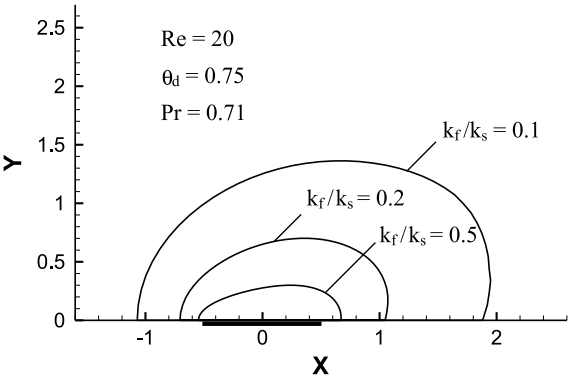

Fig. 7. Effects of the ratio of thermal conductivities on shape design, at $Re = 20$, $\theta_d = 0.75$, and $Pr = 0.71$.

Therefore, typically the 41×21 (solid)/41×101 (fluid) grid system is employed in this study.

Effects of the dominate dimensionless parameters, including θ_d, k_f/k_s, and Re, have been investigated, and the results are displayed in the following. Fig. 5 conveys the effects of the desired outer surface temperature (θ_d) on the shape design at $Re = 20$, $k_f/k_s = 1$, and $Pr = 0.71$. In this figure, the designed shapes for $\theta_d = 0.2$, 0.38, and 0.6 are shown. The obtained shape profiles clearly reflect the influence of θ_d. A higher value of θ_d leads to a smaller solid medium as expected. This is because the outer surface of higher temperature is expected to be closer to the heating element imbedded in the solid medium.

Designs for the outer surface profiles at various Re for the case at $k_f/k_s = 0.1$, $\theta_d = 0.85$, and $Pr = 0.71$ are presented in Fig. 6. Note that the size of the outer surface profile for a fixed outer surface temperature is decreased by an increase in Re. The decrease in the size of the outer surface represents a higher temperature gradient developed within the solid medium in balance with the higher heat convection associated with a higher Reynolds number. In this figure, cases at $Re = 5$, 20, and 40 are considered.

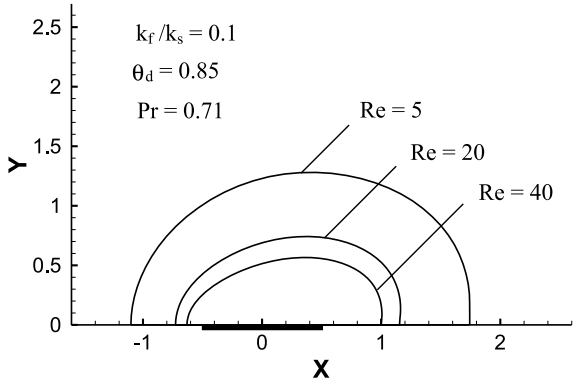

Fig. 6. Effects of Reynolds number on shape design, at $k_f/k_s = 0.1$, $\theta_d = 0.85$, and $Pr = 0.71$.

Effects of the ratio of thermal conductivities (k_f/k_s) on the shape design are investigated, and the results for $Re = 20$, $\theta_d = 0.75$, and $Pr = 0.71$ are provided in Fig. 7. For the case considered in Fig. 7, the value of k_f/k_s is set to be 0.1, 0.2, and 0.5. Results show that the size of the solid domain is decreased as k_f/k_s is increased. Note that a higher value in k_f/k_s represents a stronger heat diffusion in the fluid region. For a fixed outer surface temperature (in this case, $\theta_d = 0.75$), when the value of k_f/k_s is increased, the solid region shrinks to a smaller size for producing a higher temperature gradient in balance with the stronger heat diffusion in the fluid region.

Fig. 8 shows the convergence process of shape design for the case at $Re = 20$, $k_f/k_s = 0.1$, $\theta_d = 0.75$, and $Pr = 0.71$. It is observed that starting from a smaller initial domain (a cylinder of unit dimensionless radius), the optimization process attains the final shape in about 50 iterations. The flow fields and the nodal point distributions on the outer surface of the solid medium for the iterations are indicated. Notice that the extent of the flow vortex in the wake also grows as the size of the iterative solid domain expands during the optimization process. The adjustment of the shape profile is performed automatically by using the conjugate gradient method coupled with the redistribution method. Note that the nodal point distributions on the outer surface of the solid medium are always controlled by the redistribution method until the updated solution meets the convergence criterion. In this manner, the iterative shape profiles can keep smooth toward the end of the optimization process.

Fig. 9 shows the relative performance of the shape design for a solid medium covering a heating element

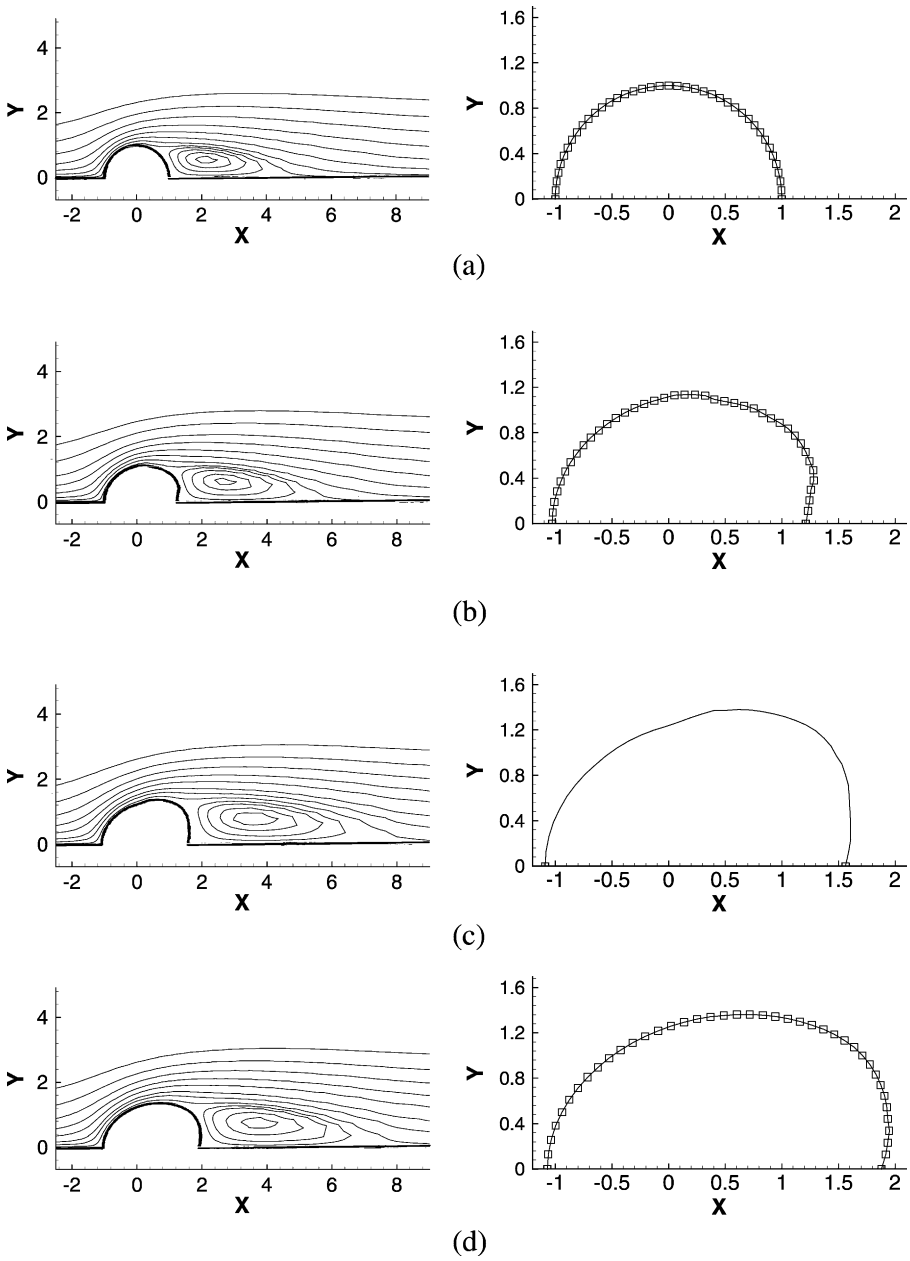

Fig. 8. Convergence of shape design process, at $Re = 20$, $k_f/k_s = 0.1$, $\theta_d = 0.75$, and $Pr = 0.71$. (a) Initial guess, (b) 6th iteration, (c) 24th iteration, and (d) final solution.

and featuring an isothermal outer surface. Plotted in the left portion of Fig. 9 are the flow pattern, the temperature distribution in both the solid and the fluid regions, and the outer surface temperature profile for the case with a circular solid medium. Notice that the outer surface temperature is varied significantly along the surface of the solid medium, and a peak value is found in the rear area of the circular cylinder. However, by applying the shape design method, a solid medium with designed outer surface profile meeting the thermal requirement for a uniformly isothermal outer surface is obtained. The results for the shape-designed solid medium are given in the right portion of Fig. 9 for comparison. It is found that the shape design for the solid

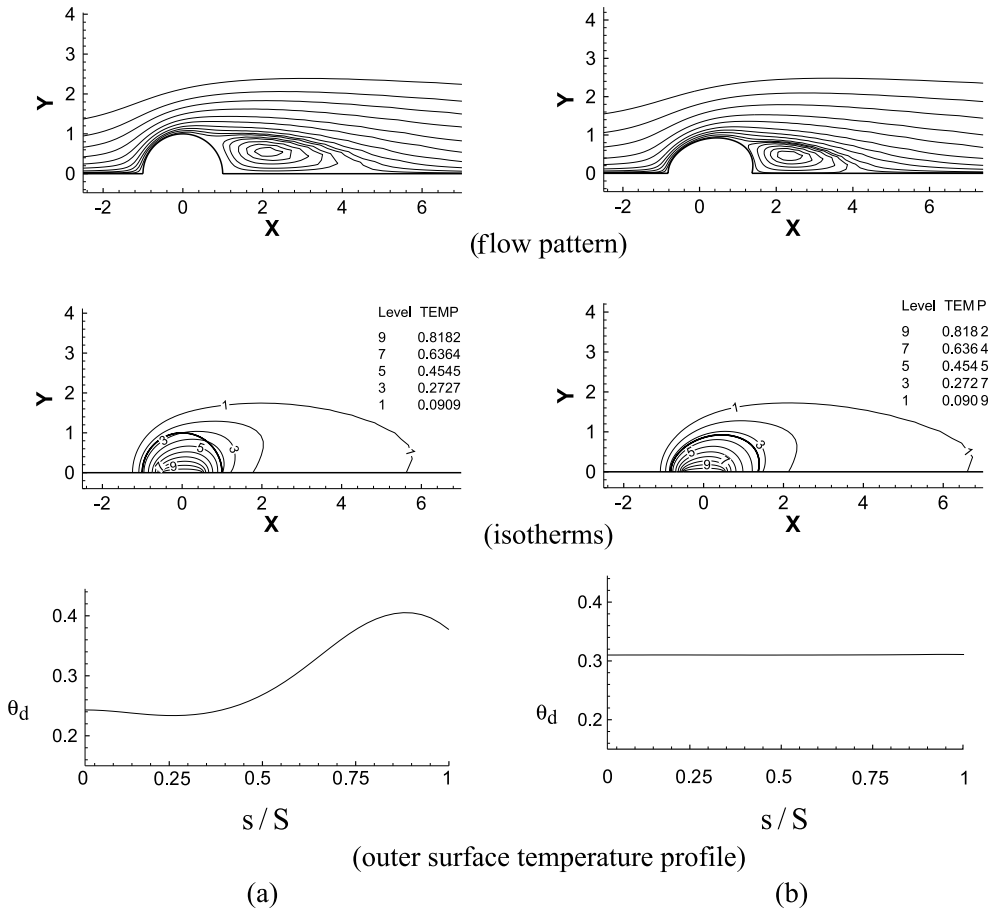

Fig. 9. Comparison in flow pattern and temperature distribution between the flows over a circular solid medium and a medium with designed shape, at $Re = 20$, $k_f/k_s = 1$, and $Pr = 0.71$. (a) A circular solid medium and (b) a shape-designed solid medium (at $\theta_d = 0.31$).

medium leads to a perfectly uniform temperature distribution on the outer surface whose outer surface temperature (θ_d) is specified by 0.31.

The efficiency of the shape design method can also be evaluated based on the relative error between the outer surface temperature of the designed solid medium ($\theta_{si,M}$) and the desired outer surface temperature (θ_d). The relative error at grid i on the outer surface, ε_i, is defined by

$$\varepsilon_i = \left|(\theta_{si,M} - \theta_d)/\theta_d\right| \tag{16}$$

The magnitude of ε_i indicates the deviation of the designed from the desired temperature distributions on the outer surface grid i.

Fig. 10 shows the data for ε for the cases considered in Fig. 5. It is found that for $\theta_d = 0.2$, the maximum absolute value of ε is approximately 0.005; however, the deviation is greatly reduced as θ_d is increased.

4. Concluding remarks

The present study is concerned with the application of the inverse heat transfer approach combining the curvilinear grid generation, the direct problem solver, the conjugate gradient method, and the redistribution method [18,19] for shape design problem.

The inverse heat transfer approach for shape design is extended to the convection problems. Shape design for the outer surface profile of a solid medium in a crossflow that contains a heating element and features an isothermal outer surface has been carried out as a test problem. Practical cases under different combinations of the dominant parameters, including Reynolds number (Re), thermal conductivity ratio (k_f/k_s), and desired outer surface temperature (θ_d), X are studied to demonstrate the performance of the approach. It is found that the optimization process leads to satisfaction in the shape

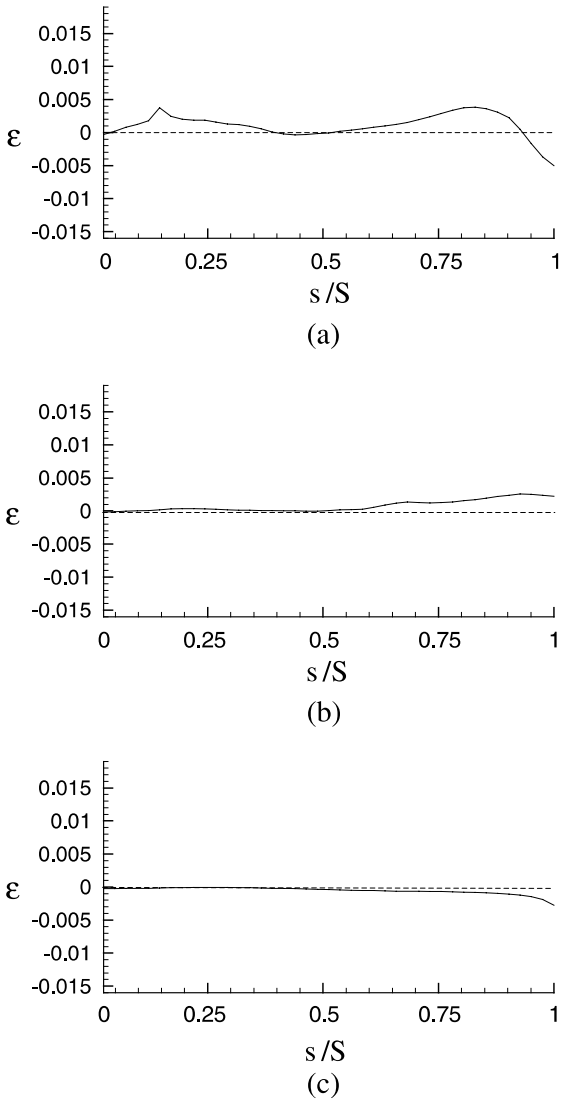

Fig. 10. Relative error of the outer surface temperature of the designed solid medium from the respective specified values, at $Re = 20$, $k_f/k_s = 1$, and $Pr = 0.71$. (a) $\theta_d = 0.2$, (b) $\theta_d = 0.38$, and (c) $\theta_d = 0.6$.

design for the isothermal outer surface profile. The relative error between the outer surface temperature of the designed solid medium and the desired outer surface temperature is in general much less than 0.005 for the typical cases considered in this study.

References

[1] G.Jr. Stolz, Numerical solutions to an inverse problem of heat conduction for simple shape, J. Heat Transfer 82 (1960) 20–26.

[2] T.J. Mirsepassi, Heat-transfer charts for time-variable boundary conditions, Br. Chem. Eng. 4 (1959) 130–136.

[3] T.J. Mirsepassi, Graphical evaluation of a convolution integral, Math. Tables Other Aides Comput. 13 (1959) 202–212.

[4] N.V. Shumakov, A method for the experimental study of the process of heating a solid body, Soviet Phys.-Tech. Phys. (Translated by American Institute of Physics) 2 (1957) 771–781.

[5] C.H. Huang, C.W. Chen, A boundary-element-based inverse problem of estimating boundary conditions in an irregular domain with statistical analysis, Numer. Heat Transfer, Part B 33 (1998) 251–268.

[6] M. Prud'homme, T.H. Nguyen, On the iterative regularization of inverse heat conduction problems by conjugate gradient method, Int. Comm. Heat Mass Transfer 25 (1998) 999–1008.

[7] C.H. Huang, S.P. Wang, A three-dimensional inverse heat conduction problem in estimating surface heat flux by conjugate gradient method, Int. J. Heat Mass Transfer 42 (1999) 3387–3403.

[8] H.M. Park, O.Y. Chung, An inverse natural convection problem of estimating the strength of a heat source, Int. J. Heat Mass Transfer 42 (1999) 4259–4273.

[9] C.H. Huang, M.N. Ozisik, B. Sawaf, Conjugate gradient method for determining unknown conduct conductance during metal casting, Int. J. Heat Mass Transfer 35 (1992) 1779–1786.

[10] P. Terrola, A method to determine the thermal conductivity from measured temperature profiles, Int. J. Heat Mass Transfer 32 (1989) 1425–1430.

[11] T.P. Lin, Inverse heat conduction problem of simultaneously determining thermal conductivity, heat capacity and heat transfer coefficient, Master thesis, Department of Mechanical Engineering, Tatung Institute of Technology, Taipei, Taiwan 1998.

[12] U. Kirsch, Efficient reanalysis for topological optimization, Struct. Optim. 6 (1993) 143–150.

[13] H. Rodrigues, P. Fernandes, A material based model for topology optimization of thermoelastic structures, Int. J. Numer. Meth. Eng. 38 (1995) 1951–1965.

[14] G. Fabbri, A genetic algorithm for fin profile optimization, Int. J. Heat Mass Transfer 40 (1997) 2165–2172.

[15] G. Fabbri, Heat transfer optimization in internally finned tubes under laminar flow conditions, Int. J. Heat Mass Transfer 41 (1998) 1243–1253.

[16] G. Fabbri, Optimum profiles for asymmetrical longitudinal fins in cylindrical ducts, Int. J. Heat Mass Transfer 42 (1999) 511–523.

[17] G. Fabbri, Heat transfer optimization in corrugated wall channels, Int. J. Heat Mass Transfer 43 (2000) 4299–4310.

[18] C.H. Cheng, C.Y. Wu, An approach combining body-fitted grid generation and conjugate gradient methods for shape design in heat conduction problems, Numer. Heat Transfer, Part B 37 (2000) 69–83.

[19] C.H. Lan, C.H. Cheng, C.Y. Wu, Shape design of heat conduction problems using curvilinear grid generation, conjugate gradient, and redistribution methods, Numer. Heat Transfer, Part A 39 (2001) 487–510.

[20] R.D. Blevins, Flow-Induced Vibration, Van Nostrand Reinhold Company, New York, 1977 (Chapter 3).

[21] J.F. Thompson, F.C. Thames, C.W. Mastin, Automatic numerical generation of body-fitted curvilinear coordinate system for fields containing any number of arbitrary two-dimensional bodies, J. Comput. Phys. 15 (1974) 229–319.
[22] J.F. Thompson, F.C. Thames, C.W. Mastin, Boundary-fitted curvilinear coordinate system for solution of partial differential equation on fields containing any number of arbitrary two-dimensional bodies, NASA CR-2729, 1976.
[23] Y.T. Yang, C.K. Chen, S.R. Wu, Transient laminar forced convection from a circular cylinder using a body-fitted coordinate system, J. Thermophys. 6 (1992) 184–188.
[24] S.V. Patankar, Numerical Heat Transfer and Fluid Flow, Hemisphere, New York, 1980 (Chapter 5).
[25] S.C.R. Dennis, G.Z. Chang, Numerical solutions for steady flow past a circular cylinder at Reynolds numbers up to 100, J. Fluid Mech. 42 (1970) 471–489.